Multistage Exit of Excited Xanthone from Micelles

Nadereh Mohtat, Frances L. Cozens,† and J. C. Scaiano*

Department of Chemistry, University of Ottawa, Ottawa, Ontario K1N 6N5, Canada

Received: April 22, 1998; In Final Form: July 8, 1998

The spectroscopic changes of xanthone associated with its exit from micelles following laser excitation occur in three distinct stages. These processes are accompanied by changes in kinetic behavior and spectra. The first stage of this spectral evolution is intersystem crossing (ISC), which is followed by spectral changes in the triplet−triplet absorption spectrum that reflect an increasingly polar environment as the probe moves from the micelle interior to the micellar surface and later to the aqueous bulk phase. In the case of sodium dodecyl sulfate micelles, these three processes occur with lifetimes of 55 ps (ISC), 3.2 ns, and 0.6 μs; the last two are assigned to diffusion toward the micelle−water interface and actual exit into the aqueous phase, respectively.

The reactivity of many organic molecules in supramolecular assemblies is frequently determined by the dynamics with which the reactants enter and exit from a given organized structure. As a result, the kinetics of these entry/exit processes have been the subject of considerable interest. For example, in the case of micelles, the exit dynamics have been studied for 2 decades. In 1979, Almgren and Thomas[1] reported a seminal study of the dynamics of arenes in micellar systems. While there are many variations of the methodology developed in this study, they frequently involve quenching of an excited state by a molecule that is only soluble in one of the pseudophases in a micellar system. For example, nitrite ions are excellent triplet quenchers and are convenient substrates for anionic micellar systems,[2] since Coulombic repulsion tends to minimize any interactions with the micellized probe molecule. Thus, at sufficiently high concentration of the aqueous quencher, the lifetime of the excited probe molecule is determined by its rate constant for exit from the micelle into the quencher-loaded aqueous phase. Studies of this type, and numerous variations of the same strategy, have led to a wealth of information on exit rate constants (mostly for the excited states of the molecule) and a limited number of entry rate constants. For the latter, the rates for hydrophobic molecules are frequently within an order of magnitude of the diffusion limit.[3−6]

It has been recognized that the interior of the micelle, the micellar surface, and the bulk aqueous phase constitute widely different environments; however, from a kinetics perspective, the exit process has generally been viewed as a single (kinetic) step readily defined by an exit rate constant, k_{-}. For most purposes, this is quite adequate and reflects satisfactorily the dynamics of probe exit, regardless of the events that precede exit into the aqueous phase and effectively "prepare" the probe for this transition.

We are interested in the detailed processes involved in micellar exit. We have selected as a probe the triplet state of xanthone, a molecule that we have frequently employed as a probe in work involving laser flash photolysis techniques.[2,7−11] The triplet state of xanthone is relatively long-lived (several microseconds) in most polar solvents, where the triplet state has π,π^* character.[9,12] The triplet−triplet absorption of xanthone shows a characteristic shift with the solvent polarity[9,10,13] and thus can be used as a sensor for this property. In our studies we have monitored the time evolution of the triplet xanthone spectrum; from these changes, we try to rationalize the events that occur following excitation of xanthone in micellar solution. To study these changes, we have employed a combination of picosecond and nanosecond laser photolysis techniques.

Experimental Section

Materials. Xanthone (Aldrich) was recrystallized from ethanol. Sodium dodecyl sulfate (SDS) (Fluka, microselect), sodium *n*-decyl sulfate (SDecS) (Lancaster), sodium *n*-tetradecyl sulfate (STDS) (Lancaster), and hexadecyltrimethylammonium chloride (CTAC) (Kodak) were used as received. Cupric sulfate (BDH chemicals) and sodium nitrite (Fisher Scientific) were also used as received. Water was purified through a Millipore MilliQ system.

Nanosecond Laser Flash Photolysis. Samples of 0.1 mM xanthone were nitrogen saturated in aqueous solutions of 0.1 M SDS, 0.05 M SDecS, 0.01 M STDS, or 0.06 M CTAC. Sodium chloride (0.2 and 0.3 M) was added to 0.1 and 0.05 M SDS, respectively, prior to the addition of xanthone. Solutions for recording the transient spectra were made to flow through a 7×7 mm^2 Suprasil quartz cell, which held 2 mL. However, static samples were used for the quenching experiments. The samples were excited by pulses of a Surelite Nd:YAG laser (<25 mJ per 8 ns pulse) using the third harmonic, 355 nm. The signals from the monochromator/photomultiplier system were initially captured by a Tektronix 2440 digitizer and transferred to a PowerMacintosh computer that controlled the experiment with software developed in the LabVIEW 3.1.1 environment from National Instruments. Other aspects of the system are similar to those described earlier.[9,14]

Picosecond Laser Flash Photolysis. The picosecond transient absorption studies were carried out using 35 ps pulses from a Continuum PY-61 Nd:YAG laser. The experimental setup has many features similar to those already described in the literature.[15] The fundamental, 1064 nm (30 mJ) 35 ps laser pulse of the Nd:YAG laser was sent through two internal harmonic generators to give the excitation beam (355 nm, ≤5

† Present address: Department of Chemistry, Dalhousie University, Halifax, Nova Scotia B3H 4J3, Canada.

S1089-5647(98)01951-8 CCC: $15.00 © 1998 American Chemical Society
Published on Web 09/01/1998

mJ × pulse^{-1} , ≤35 ps). After exiting the laser, the excitation beam was directed with a series of dichroic mirrors to the sample cell. The probe or monitoring beam was generated by directing a small amount (4 mJ) of the 1064 nm beam through a series of lenses into an external amplifier. The output from the external amplifier was around 30 mJ and was controlled by an adjustable power supply. The amplified 1064 nm light was then directed with a series of dichroic mirrors to a retroreflector mounted on a computer-controlled precision rail table. The light exiting the retroreflector was focused using a 20 cm focal length lens into a 20 cm long cell with quartz entrance and exit windows containing a 1:1 mixture of H_2O/D_2O with 5% (by weight) P_2O_5. Focusing of the 1064 nm light into the H_2O/D_2O solution causes the phenomenon known as continuum generation, whereby white light ranging from 400 to 800 nm and having a pulse width of ca. 35 ps is emitted from the cell. The white light is then sent through a diffuser in order to mix the spectral colors and focused onto a 1 ft bifurcated quartz fiber-optic cable. The fiber-optic cable carries one-half of the monitoring light to the sample cell and the other half to the reference cell; the latter is equipped with a variable neutral density filter. The two beams of white light are sent via a focusing lens through a sample and a reference cell to a second set of fiber-optic cables that brings the light to a spectrograph. In the spectrograph, the white light is separated into its individual wavelengths and directed into a Princeton Instruments intensified dual diode array spectrometer. The data from both the sample diode array and the reference diode array are sent to a Princeton Instruments controller (ST-120), which is interfaced to a Macintosh Quadra computer that allows experiment control and data processing with software developed in the LabVIEW 3.1.1 environment from National Instruments.

By use of this system, absorption spectra are obtained by carrying out two acquisitions. The first is one in which the monitoring light is sent through the reference and sample cells via the bifurcated quartz fiber-optic cable and the excitation beam is directed onto the sample. During this acquisition, our transient of interest is generated and detected. The second acquisition is used as a reference that corrects for any differences in the sample and reference monitoring beams. This is carried out by measuring the intensity of the monitoring beams through the sample and reference cells in the absence of the excitation pulse. In addition, fluorescence and the background counts are also corrected for during the course of an experiment. For signal averaging, up to 200 transient acquisitions were made at 10 Hz, followed by an identical number of reference, fluorescence, and background acquisitions.

Transient decay traces are generated by measuring the absorption spectrum of the transient at specific delay times after excitation. The time delay was adjusted by using the computer-controlled rail table, which changes the path length of the 1064 nm light in relation to the excitation pulse. This changes the time at which the monitoring beam hits the sample and reference cells relative to the time the excitation pulse hits the sample and reference cells. Absorption spectra are recorded at many different time delays. At each time delay, the intensity of the absorption at the wavelength of interest was calculated using a program that measures the area under a selected wavelength range. The decay trace is then constructed by plotting absorption intensity versus time for the selected wavelength.

Picosecond Fluorescence. The third harmonic (355 nm, ca. 0.5 mJ, ≤35 ps pulse) of the same Continuum PY61-10 Nd:YAG laser system mentioned above was used for excitation, with a Hamamatsu streak scope C4334 for time-resolved fluorescence detection. With deconvolution analysis it is possible to determine fluorescence lifetimes as short as ∼15 ps. For fluorescence lifetimes above 50 ps, typical errors are <3% for the main emission component, while shorter lifetimes can have as much as 10% error. Long lifetimes for minor components can have considerable error (±100 ps).

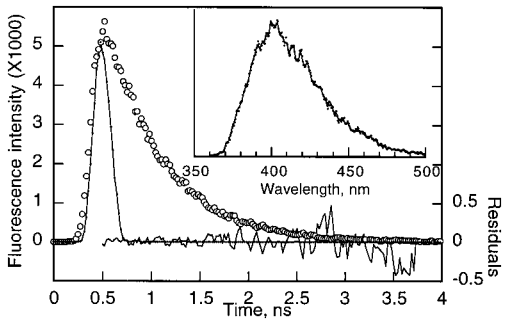

Figure 1. Fluorescence decay for 0.1 mM xanthone in water (λ_{max} ∼400 nm) and the normalized instrument response function. Residuals are shown on the right scale. The inset shows the emission spectrum from aqueous xanthone following 355 nm laser excitation.

TABLE 1: Singlet Lifetime of ∼0.1 mM Xanthone in Various Environments, Based on Fluorescence Measurements

solvent	singlet lifetimes (ps)	fraction contribn
water	600	0.99
acetonitrile	<30	
isopropanol	<30	
SDS	67	0.90
	236	0.10
SDecS	36	0.90
	450	0.10
STDS	92	0.90
	668	0.10
CTAC	90	0.90
	730	0.10
SDS + 0.2 M NaCl	127	0.94
	454	0.06
SDS + 0.3 M NaCl	149	0.96
	1260	0.04

Results

Xanthone is not fluorescent in typical organic solvents, such as acetonitrile or 2-propanol. The behavior is characteristic of many aromatic ketones (e.g., benzophenone) that undergo fast and efficient intersystem crossing. Typical singlet lifetimes for xanthone in organic solvents are around 10 ps.[16] In aqueous systems, xanthone shows moderate fluorescence; in pure water, the emission is monoexponential with a lifetime of 600 ps and a fluorescence maximum at ∼405 nm (Figure 1). In micellar solution, the fluorescence decay is generally much shorter than in water and follows biexponential decay, with the short component dominating the decay (typically ∼90%). The long component has a lifetime consistent with that determined in pure water, given the relatively large errors that characterize this minor contribution (≤10%). The data are summarized in Table 1.

Picosecond laser excitation of xanthone in SDS (0.1 M) micellar solution leads to the transient spectrum of Figure 2. As time passes, the maximum of this spectrum shifts toward shorter wavelengths, normally indicative of an increase in environmental polarity.[9] The position of the maximum absorbance (λ_{max}) was determined by fitting the top of the absorption band to a Gaussian function, as shown in Figure 2.[17] While the shifts were evident without any need to resort to this analysis,

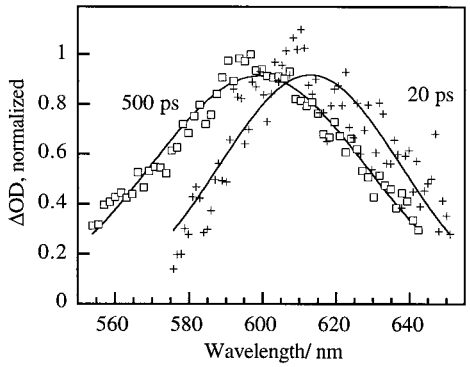

Figure 2. Transient spectra for triplet xanthone (0.1 mM in 0.1 M SDS) illustrating the Gaussian fit (see text) at two different delay times.

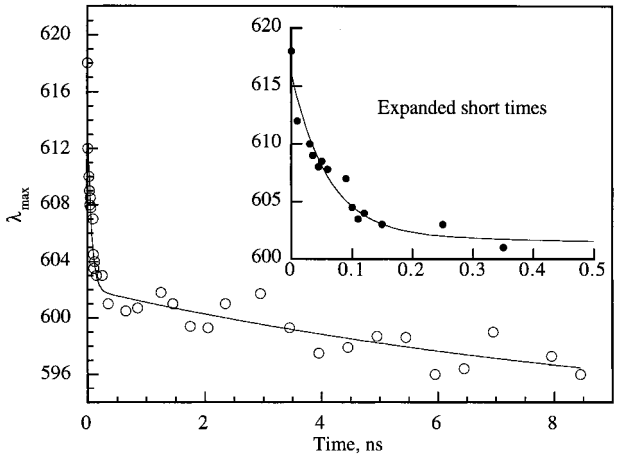

Figure 3. Evolution of λ_{max} with time following 355 nm picosecond laser excitation of 0.1 mM xanthone in 0.1 M SDS, with the λ_{max} determined as shown in Figure 2. The inset shows an expansion of the data up to 500 ps delay.

we felt that this approach eliminated any subjective component in the determination of λ_{max}, making it independent of the person analyzing the data. While the details of spectral evolution are presented below, it is worth summarizing the nature of those changes. In all cases, we find a rapid spectral change occurring typically around 100 ps. This is followed by a second process, occurring predominantly in 1−50 ns range. We note that these times are too short for true micellar exit to occur.[2] Spectral changes in the nanosecond and microsecond time scale are small, although actual exit into the aqueous phase occurs in this time domain (vide infra). Analysis of data from a series of spectra acquired at different times following picosecond laser excitation led to the time evolution of Figure 3; this figure is representative of those obtained under a variety of conditions and for several surfactants.

The data in Figure 3 were analyzed with a double exponential function, forcing the infinite level to the λ_{max} position recorded at early times in the nanosecond experiments (λ^{∞}_{max}), that is,

$$\lambda^{t}_{max} = (\lambda^{0}_{max} - \lambda^{\infty}_{max})(a_1 e^{-k_1 t} + a_2 e^{-k_2 t}) \qquad (1)$$

where λ^{0}_{max} is the earliest value (<35 ps) recorded after laser excitation, k_1 and k_2 are rate constants for spectral evolution, and the preexponential parameters a_1 and a_2 indicate the fraction of picosecond spectral evolution that is associated with k_1 and k_2, respectively. Analysis of the data in Figure 3 according to this method yields $k_1 = 1.8 \times 10^{10}$ s^{-1} and $k_2 = 3.1 \times 10^{8}$ s^{-1}. Most of the spectral evolution is associated with the faster process, as indicated by the fact that $a_1 > a_2$ in all cases (see Table 2). The fast rate constant (k_1) corresponds to a lifetime of ∼55 ± 10 ps for SDS. The second, slower process is subject to considerably larger error as a result of the small spectral change occurring during this phase of the process and the somewhat weaker signals at longer times. For the system of Figure 3, the slow component has $\tau_2 = 3.2 \pm 1$ ns.[18] Similar analyses for the other surfactant systems examined have led to the data in Table 2. We note that the physical dimensions of our picosecond transient absorption system limit the time monitored to a maximum of ∼9 ns. Thus, lifetimes exceeding ∼20 ns become unreliable; for these systems, we have indicated $k_2 < 5 \times 10^7$ s^{-1}.

TABLE 2: Picosecond Data for the Evolution of the Spectral Characteristics of the Xanthone Triplet in Micellar Solution

system[a]	k_1	a_1	k_2	a_2
SDecS	1.55×10^{10}	0.94	104×10^{7}	0.06
SDS	1.82×10^{10}	0.71	31×10^{7}	0.29
SDS + 0.2 M NaCl	5.31×10^{9}	0.67	5.5×10^{7}	0.33
SDS + 0.3 M NaCl	5.76×10^{9}	0.86	$<5 \times 10^{7}$	0.14
CTAC	1.09×10^{10}	0.63	$<5 \times 10^{7}$	0.37
STDS	1.57×10^{10}	0.88	20×10^{7}	0.12

[a] Abbreviations: SDecS, sodium *n*-decyl sulfate; SDS, sodium dodecyl sulfate; STDS, sodium tetradecyl sulfate; CTAC, cetyltrimethylammonium chloride.

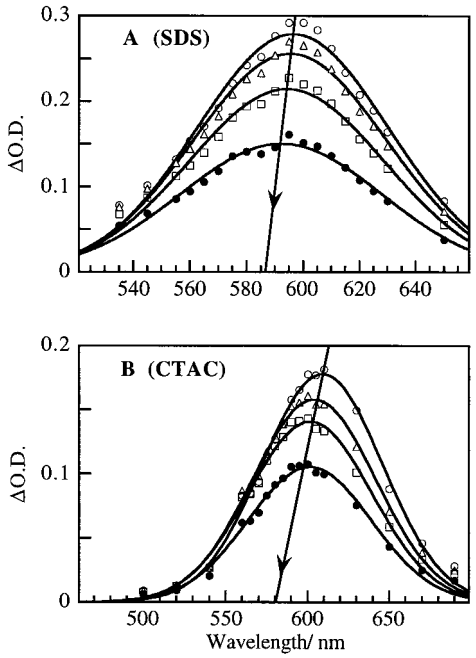

Figure 4. Nanosecond transient absorption spectra from 0.1 mM xanthone following 355 nm laser excitation after various delay times during triplet decay. (A) in 0.1 M SDS (32, 120, 320, and 790 ns) and (B) in 0.05 M CTAC (50, 160, 340, and 800 ns). The data were fitted with Gaussian functions as explained in the text, and the linear fits correspond to the best line through the calculated maxima.

In addition to several surfactants with varying chain lengths, we also examined the effect of added salt, which is known to lead to larger micelles.[19] These data are also presented in Table 2. The effect of 0.2 or 0.3 M salt is virtually the same.

The two processes examined with picosecond techniques are too fast to correspond to the exit of xanthone into the aqueous phase. Typically these processes occur with rate constants slightly over 10^6 s^{-1} for ketones of similar size.[2] Studies were carried out with nanosecond techniques, also using 355 nm for excitation. The spectral changes that occur as the triplet state decays in this time scale are small and difficult to monitor (see

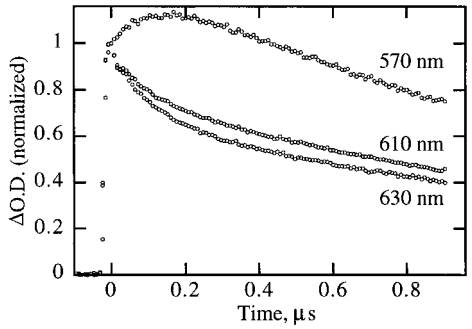

Figure 5. Transient traces recorded at various wavelengths following 355 nm nanosecond laser excitation of 0.1 mM xanthone in 0.06 M CTAC solution.

Figure 4). The case of the positive surfactant CTAC shows the most readily detectable changes. In fact, in this particular system it is also possible to detect the changes in the traces recorded at some wavelengths (see Figure 5); for example, the shape of the 570 nm trace could not be explained by simple arguments relating to triplet decay and requires a concurrent spectral evolution. In Figure 4, we have joined the maxima at different times (determined using a Gaussian function, as in the picosecond experiments) with a straight line to help visualize this small shift. While the trend toward a more *aqueous* environment follows that observed in the picosecond time scale (see Table 3), there is clearly too limited information to base the nanosecond−microsecond kinetic analysis on modest spectral shifts. It is worth noting that spectral extrapolation to long time scales does not lead to the same λ_{max} with all surfactants, and the value of λ^{∞}_{max} (typically ∼595 nm) is larger than that for water (around 584 nm). This is a clear indication that exit does not lead to a completely aqueous environment for the probe, but rather, an exit/entry equilibrium is established, such that the observable λ^{∞}_{max} is a composite of contributions from the micellar and aqueous environments. If an aqueous-only quencher is added to the solution, this molecule will only be able to quench excited probes that have fully exited from the micelles. For example, for anionic micelles, nitrite ions are a good choice,[2] and at the moderate concentrations employed (vide infra) there is little chance of quencher penetration into the micelle. Scheme 1 shows the mechanism for excitation, exit/entry, and quenching,

Scheme 1

$$X_m \xrightarrow{h\nu} \xrightarrow{ISC} X^*_m \quad (2)$$

$$X^*_m \xrightarrow{k^m_o} X_m \quad (3)$$

$$X^*_m \xrightarrow{k_-} X^*_w + M \quad (4)$$

$$X^*_w + M \xrightarrow{k_+} X^*_m \quad (5)$$

$$X^*_w + Q \xrightarrow{k_q} X_w + P \quad (6)$$

$$X^*_m + Q \xrightarrow{k_{qm}} X_m + P \quad (7)$$

P = Q, Q*, or products

where X is xanthone, the subscripts 'm' and 'w' refer to the micellar and aqueous phases, respectively, and 'M' is the micellar concentration calculated taking into account the critical micelle concentration (cmc) and aggregation number for each particular system.[20] Scheme 1 leads to the expression of eq 8,[5,21,22]

$$k_{expt} = k^m_o + k_- + k_{qm} - \frac{k_- k_+[M]}{k_+[M] + k^w_o + k_q[Q]} \quad (8)$$

where k_{expt} is the rate constant for xanthone triplet decay and k^m_o and k^w_o represent triplet decay in the two phases in the absence of quencher. At sufficiently high aqueous quencher concentration, the last two terms vanish and the value of k_{expt} reaches a plateau given by $k^m_o + k_-$ from which the exit rate constant can be readily obtained. Under these conditions, the excited probes are quenched as soon as they exit, with no probability for re-entry. The inset in Figure 6 shows a representative plot of this type. Even in the best of cases, the plateau is not perfectly defined. The plot also relies heavily on the worst data; that is, that obtained at high quencher concentrations and where the lifetimes are shortest. We assume that nitrite ions are exclusively located in the aqueous phase, this being the only region in which quenching takes place after the molecular exit process is complete. Further, we assume that k^w_o is small, which is confirmed experimentally. On this basis, eq 8 simplifies to eq 9

$$k_{expt} - k^m_o = k_- - \frac{k_- k_+[M]}{k_+[M] + k_q[Q]} \quad (9)$$

A linear form of eq 9 should be preferred for experiments of this type, as shown in eq 10

$$(k_{expt} - k^m_o)^{-1} = \frac{1}{k_-}\left[1 + \frac{k_+[M]}{k_q[Q]}\right] \quad (10)$$

TABLE 3: Evolution of the Position of λ_{max} (nm) in the Picosecond and Nanosecond Time Scales

system	λ^0_{max}	λ^{300ps}_{max}	$\lambda^{8\,ns}_{max}$	$\lambda^{40\,ns}_{max}$
SDecS	609	602	596	596
SDS	618	602	597	597
SDS + 0.2 M NaCl	614	605	602	599
SDS + 0.3 M NaCl	615	602	599	597
CTAC	623	618	615	609
STDS	615	601	597	597

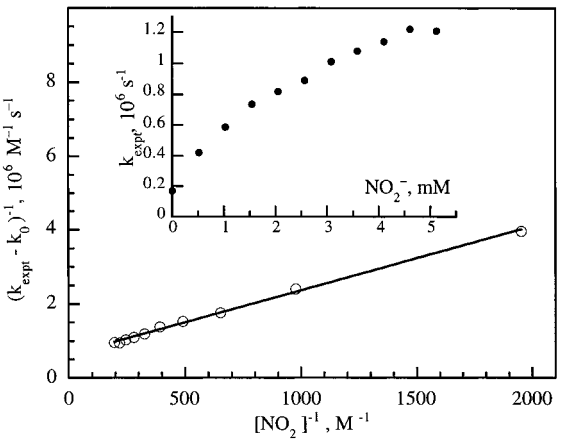

Figure 6. Quenching plot for xanthone triplets interacting with nitrite ions in 0.1 M SDS solution following laser excitation at 355 nm. The main figure is plotted according to eq 10, while the inset shows the variation of the observed rate constant for triplet decay against the nitrite concentration.

TABLE 4: Exit and Entry Data Based on Quenching Studies in the Nanosecond/Microsecond Time Scale

system	quencher	k_- (s^{-1})	k_+/k_q (M^{-1})	k_+ ($M^- s^{-1}$)
SDecS	$Na(NO_2)$	2.70×10^6	3.69	2.40×10^{10}
SDS	$Na(NO_2)$	1.56×10^6	1.83	1.19×10^{10}
		or 1.71×10^6	2.42	1.57×10^{10}
		2.7×10^6 (ref 2)		
SDS + 0.2 M NaCl	$Na(NO_2)$	2.66×10^6	~2.8	$\sim 1.8 \times 10^{10}$
SDS + 0.3 M NaCl	$Na(NO_2)$	2.12×10^6	2.29	1.49×10^{10}
CTAC	$Cu(SO_4)$	0.58×10^6	9.97	0.86×10^9
STDS	$Na(NO_2)$	1.07×10^6	1.11	7.19×10^9

The main part of Figure 6 shows representative plots according to eq 10 from which we obtain the exit rate constants k_- and the ratio k_+/k_q. The value of k_q can be determined independently, since it corresponds to the quenching of xanthone triplets by nitrite in aqueous solution. This value has been measured as 6.5×10^9 M^{-1} s^{-1}. The data obtained from nanosecond experiments are summarized in Table 4. As expected, exit rate constants are significantly slower than the k_1 and k_2 values obtained in the picosecond experiments. The values of k_- are in line with those expected from studies in related systems.

In a control experiment, we examined the picosecond spectroscopy of the xanthone triplet in water. Despite its very limited solubility, it is possible to achieve optical densities of around 0.1 at 355 nm (the laser wavelength). The maximum stayed at 584 ± 2 nm from 50 ps to 8 ns after laser excitation and agrees well with the position observed in the microsecond time scale, thus showing also that both laser instruments (nanosecond and picosecond) yield consistent spectral values.

Discussion

Three distinct processes follow excitation of xanthone in micellar solution, ultimately leading to the exit of xanthone triplets into the aqueous phase. The values of exit and entry rate constants are such that under most experimental conditions, an equilibrium is established with significant fractions of xanthone triplets in both phases. As a result, the position of λ_{max} at long times does not coincide with that for xanthone in water. The values of k_1, k_2, and k_- are summarized in Tables 2 and 4. What processes at the molecular level are associated with these rate constants? The slowest value (i.e., k_-) is straightforward, since it is clearly this process that makes the xanthone triplet readily accessible to an aqueous quencher; thus, k_- must correspond to the actual exit from the micelle into the aqueous phase. We believe that k_1 and k_2 are associated with processes that precede actual exit.

Carbonyl compounds with low lying triplets with π,π^* character, as is the case for xanthone in polar media, generally undergo a large increase in dipole moment upon excitation.[23] In the case of xanthone, this characteristic has been used to advantage in a number of systems. In particular, in the case of cyclodextrin complexes[10,13] and of surfactant−polyelectrolyte aggregates[11] in aqueous solution, the triplet state of xanthone tends to exit toward the aqueous phase following the high increase in polarity that accompanies excitation. Since polarity changes are also accompanied by changes in λ_{max} for the triplet−triplet absorption, the consequence is that following excitation, xanthone exits the supramolecular system, a process that is accompanied by a decrease in λ_{max}. Bohne et al. have recently employed these concepts to study both entry and exit from the cyclodextrin cavity.[13] Typically, exit occurs in the 10^{-7} s time scale.[10,13] Similar concepts are employed in this study. Thus, the spectral changes observed for xanthone triplets in the picosecond time scale reflect an increasingly polar environment, as judged by the decrease in the λ_{max} value.

We believe that k_1 is associated with the decay of the excited singlet state of xanthone, which predominantly occurs by intersystem crossing to the triplet state. The lifetimes for this process, (i.e., ~55 ps for SDS; see Table 1), as determined from the time evolution of the spectrum, are in reasonable agreement with the fast component of the fluorescence (67 ps for SDS). In this phase of the process the likely cause of the spectral shift is the changing composition of the singlet−triplet mixture as intersystem crossing occurs; it is not unusual for the absorption of singlets to be red-shifted with respect to triplets. The fact that the lowest value of a_1 was obtained for CTAC (see Table 1) can be taken as an indication of the very low fraction of xanthone present in the water phase in the case of this surfactant. Possibly, as the excited-state dipole is greater than that of the ground state, the relaxation of xanthone solvation water following excitation within the micelle may contribute to some degree to the spectral evolution and thus to minor differences with kinetic data acquired using fluorescence spectroscopy. Relatively slow water relaxation (nanoseconds) has been reported in reverse micelles[24,25] and in biological materials.[26]

The value of k_2 falls within the time scale of intramicellar migration.[27] We believe that k_2 should be interpreted as the process that accounts for the displacement of xanthone from its original location to the surface of the micelle. Two things are worth noting: since xanthone is a moderately hydrophilic substance, its ground-state location may not be too far from the surface, and second, the surface location preferred by the solvated excited triplet state must be in a highly aqueous environment, given that λ_{max} at this time is very similar to that observed at much longer times when the exit/entry equilibrium has been established, that is, in the nanosecond laser photolysis experiments. The large CTAC micelles provide the best system to monitor the shift of the absorption in the nanosecond time scale (see Figure 4). The CTAC micelles tend to provide a relatively nonpolar environment that even near the micellar surface is rather different from that in the aqueous phase.

The position of λ_{max} immediately after picosecond excitation (Table 4) should provide a reasonable marker for the absorption maximum for the singlet state in micelles, at least for those systems having singlet lifetimes in excess of 100 ps, in which cases they are comfortably resolved by our system (35 ps resolution).

The shift associated with k_2, which we relate to the migration of excited xanthone, is typically around 5 nm, suggesting that xanthone resides in the more polar regions of the micelle even in its ground state. The small changes associated with k_2 are difficult to monitor, and k_2 is subject to more error than the other kinetic parameters reported here; however, there is no doubt that an intermediate process (between k_1 and k_-) is required, with typical lifetimes in the 10 ns time scale.

Addition of salts normally makes micelles grow and eventually change to a rodlike shape.[20] This latter change is probably not achieved in the sodium chloride concentration range employed. To our surprise, changes in λ_{max} associated with ionic strength changes are quite small. There is a change from 618 to 614 nm for λ_{max} in SDS immediately after picosecond excitation upon addition of 0.2−0.3 M salt. We were surprised that the growth of the micelle is accompanied by an increase in polarity. After the fast decay, the environment sensed by xanthone is virtually the same regardless of the salt concentration.

The effect of micellar structure on the dynamics of exit (k_-) follows the usual trend of slower exit for the bigger micelles (see Table 4). The process governed by k_2 seems to follow essentially the same order as that governed by k_-, being largest for the smaller, more 'fluid' micelles.

Acknowledgment. Thanks are owed to the Natural Sciences and Engineering Research Council of Canada for generous support in the form of a research grant (J.C.S.), a postdoctoral fellowship (F.L.C.), and a graduate scholarship (N.M.). We are also grateful to Dr. Mónica Barra for her contribution to the development of our picosecond laser system.

References and Notes

(1) Almgren, M.; Grieser, F.; Thomas, J. K. *J. Am. Chem. Soc.* **1979**, *101*, 279.
(2) Scaiano, J. C.; Selwyn, J. C. *Can. J. Chem.* **1981**, *59*, 2368.
(3) Selwyn, J. C.; Scaiano, J. C. *Can. J. Chem.* **1981**, *59*, 663.
(4) Aniansson, E. A. G.; Wall, S. N.; Almgren, M.; Hoffmann, H.; Kielmann, I.; Ulbricht, W.; Zana, R.; Lang, J.; Tondre, C. *J. Phys. Chem.* **1976**, *80*, 905.
(5) Aikawa, M.; Yekta, A.; Turro, N. J. *Chem. Phys. Lett.* **1979**, *68*, 285.
(6) Atherton, N. M.; Strach, S. J. *J. Chem. Soc., Faraday Trans. 2* **1972**, *68*, 374.
(7) Weir, D.; Scaiano, J. C. *Tetrahedron* **1987**, *43*, 1617.
(8) Wilkinson, F.; Willsher, C. J.; Casal, H. L.; Johnston, L. J.; Scaiano, J. C. *Can. J. Chem.* **1986**, *64*, 539.
(9) Scaiano, J. C. *J. Am. Chem. Soc.* **1980**, *102*, 7747.
(10) Barra, M.; Bohne, C.; Scaiano, J. C. *J. Am. Chem. Soc.* **1990**, *112*, 8075.
(11) Abuin, E. B.; Scaiano, J. C. *J. Am. Chem. Soc.* **1984**, *106*, 6274.
(12) Garner, A.; Wilkinson, F. *J. Chem. Soc., Faraday Trans. 2* **1976**, *72*, 1010.
(13) Liao, Y.; Frank, J.; Holzwarth, J. F.; Bohne, C. *J. Chem. Soc., Chem. Commun.* **1995**, 199.
(14) Scaiano, J. C.; Tanner, M.; Weir, D. *J. Am. Chem. Soc.* **1985**, *107*, 4396.
(15) Schmidt, J. A.; Hilinski, E. F. *Rev. Sci. Instrum.* **1989**, *60*, 2902.
(16) Cavaleri, J. J.; Prater, K.; Bowman, R. M. *Chem. Phys. Lett.* **1996**, *259*, 495.
(17) The Gaussian function offers a convenient way to fit the data objectively. It is not meant to imply that the spectral shape must follow a Gaussian distribution.
(18) It is rather speculative to try to transform this lifetime into an intramicellar diffusion constant; however, the assumption that the distances traveled are between 10 and 15 Å yields diffusion constants in the (1−3) $\times$ 10^{-6} cm^2 s^{-1} range.
(19) Hayashi, S.; Ikeda, S. *J. Phys. Chem.* **1980**, *84*, 744.
(20) Leigh, W. J.; Johnston, L. J. In *Handbook of Organic Photochemistry*; Scaiano, J. C., Ed.; CRC Press: Boca Raton, FL, 1989; Vol. II, p 401.
(21) Turro, N. J.; Okubo, T.; Chung, C.-J. *J. Am. Chem. Soc.* **1982**, *104*, 1789.
(22) Ju, C.; Bohne, C. *J. Phys. Chem.* **1996**, *100*, 3847.
(23) Fessenden, R. W.; Carton, P. M.; Shimamori, H.; Scaiano, J. C. *J. Phys. Chem.* **1982**, *86*, 3803.
(24) Sarkar, N.; Das, K.; Datta, A.; Das, S.; Bhattacharyya, K. *J. Phys. Chem.* **1996**, *100*, 10523.
(25) Cho, C. H.; Chung, M.; Lee, J.; Nguyen, T.; Singh, S.; Vedamuthu, M.; Yao, S.; Zhu, J.-B.; Robinson, G. W. *J. Phys. Chem.* **1995**, *99*, 7806.
(26) Mashimo, S.; Kuwabara, S.; Yagihara, S.; Higasi, K. *J. Phys. Chem.* **1987**, *91*, 6337.
(27) Jay, J.; Johnston, L. J.; Scaiano, J. C. *Chem. Phys. Lett.* **1988**, *148*, 517.